

SUPPLEMENTAL FIGURE LEGEND

Figure S1. Expression of insulin and insulin receptors during development. (A-B) real-time PCR analysis of *insulin a (insa)*, *insulin receptor a (insra)* and *insulin receptor b (insrb)* in embryos. $n=3$ for each time point. Inset graph shows magnified detail of circled region. (C-D) fluorescent *in situ* hybridization indicating the expression of *insra + insrb* (red) in pancreatic tissues, including the islet β (*ins:CFP-NTR* in C, green) and α cells (*gcga:GFP* in D, green).

Figure S2. Insulin signaling blockade via *dnIRS2-GFP* mis-expression and drug treatments. (A) Peptide sequence of *dnIRS2-GFP* transgene showing pleckstrin homology (PH), phosphotyrosine binding (PTB) and GFP domains. (B) Control and *dnIRS2-GFP* mRNA-injected embryos at 24 hours post fertilization (hpf). (C,D) *In situ* hybridization showing *pdx1* expression in control (C) and *dnIRS2-GFP* mRNA-injected (D) embryos. *pdx1* expression is expanded with insulin signaling blockade. (E,F) Confocal projections of 30 hpf *Tg(ins:CFP-NTR)* pancreatic islets treated with DMSO as a vehicle control (E) or 1 μ M wortmannin (F). (G) Quantification of β cells in DMSO-treated control ($n=10$) and 100 μ M U0126-treated ($n=9$) islets at 32 hpf. No change in β cell number was observed with U0126-mediated MAPK inhibition. Student's t-test was used to determine significance in G.

Figure S3. Pancreatic β cell mass normalizes to wild type levels at 96 hpf after continual induction of *HOT:dnIRS2*. (A-B'') Merged and single channel confocal projections of 96 hpf *HOT:dnIRS2 Cre-* control (A-A'') and *HOT:dnIRS2* (B-B'') islets after heat shock at 10 hpf, 24 hpf, 28 hpf, 32 hpf, 36 hpf, 48 hpf, 56 hpf, 72 hpf and 80 hpf. Ubiquitous induction of *dnIRS2-GFP* occurs only in the *Cre+* embryos. (C) Quantification of β cells in 96 hpf *HOT:dnIRS2 Cre-* control ($n=12$) and *HOT:dnIRS2* ($n=10$) islets; β cell mass is indistinguishable between the two conditions. Student's t-test was used to determine significance in C.

Figure S4. Knockdown of insulin via *insulin-a* morpholino (*insaMO*). (A) Diagram illustrating *insa* pre-mRNA structure in wild type and *insaMO*-injected cells. *insaMO* targets the exon 2-intron 2 boundary of *preproinsulin-a* mRNA and generates two nonsense alternative splicing products. Primers complementary to exon 1 and exon 3 amplify the differentially spliced cDNA products. (B) Agarose gel showing PCR amplified *insa cDNA* products; mRNA was extracted from control and *insaMO*-injected embryos at 2 days post fertilization (dpf). Note that

a single PCR product with size of 420 bp was detected in control embryos but two aberrant PCR products—520 and 360 bp—were detected in *insaMO*-injected embryos. β actin was used as internal control. (C) The PCR products in control and *insaMO*-injected embryos were extracted, cloned into pJet vector, and sequenced. *insaMO*-injected embryos showed two aberrant splice products: Product 1 included intronic sequence; Product 2 showed partial deletion of exon 2. (D) Predicted peptide sequence of control and two aberrant splice products. (E) No overt gross embryonic phenotypes resulted from injection of increasing doses of *insaMO* ranging from 2 ng to 8 ng.

Figure S5. Sustained absence of Insulin protein by *insaMO* at 72 and 96 hpf. Merged and single channel confocal images of 72 hpf (A-B'') and of 96 hpf (C-D'') *Tg(ins:CFP-NTR)* control (A-A'';C-C'') and *insaMO*-injected (B-B'';D-D'') islets stained for CFP (β cells, green), insulin (red) and glucagon (white). Insulin protein was undetectable in β cells at both stages.

Figure S6. Co-injection of *insa* mRNA rescues the expansion of β cells in *insaMO*-injected islets. (A-C') Merged and single channel confocal projection of 24 hpf *Tg(ins:CFP-NTR)* control (A,A'), *insaMO*-injected (B,B'), and *insaMO* + *insa* mRNA-injected (C,C') islets immunostained for CFP (β cells, green), Pdx1 (red), and DNA (blue). (D) Quantification of β cells in control, *insaMO*-injected, and *insaMO* + *insa* mRNA-injected islets. The expansion of β cell mass observed in *insaMO*-injected islets is rescued when *insa* mRNA is co-injected.

Figure S7. Knockdown of *insb* results in severe developmental defects. (A) Diagram illustrating *insb* pre-mRNA structure in wild type and *insbMO*-injected cells. *insbMO* targets the exon 4-intron 4 boundary of *preproinsulin-b* mRNA and promotes the deletion of exon 4. Primers complementary to exon 3 and exon 5 amplify the differentially spliced cDNA products. (B) Agarose gel showing amplified *insb* PCR product from 2 dpf control and *insbMO*-injected embryos. Note that a PCR product with a size of 427 bp was detected in control embryos (arrowhead) but not *insbMO* injected embryos. A weak product of 210 bp can be detected in *insbMO*-injected embryos (arrow). β actin was used as an internal control. (C) Dose dependent phenotypes at 48 hpf after *insbMO* injection. Arrow indicates head defect first observed at 2 ng *insbMO* dose. (D,E) RT-PCR analysis of cDNA in 30 hpf *insbMO*-injected (D) and *insaMO*-injected (E) embryos. Neither *insbMO* nor *insaMO* affected the splicing or expression of the mRNA of the respective paralog. (F-G') Merged and single channel confocal planes of 24 hpf

control (F,F') and *insbMO*-injected (G,G') islets of *Tg(ins:CFP-NTR)* embryos stained for CFP (β cells, green) and insulin (red). (H) Quantification of *ins:CFP-NTR*⁺ β cells in 24 hpf control ($n=5$) and *insbMO*-injected embryos ($n=6$). Student's t-test was used to determine significance in H.

Figure S8. Treatment of PI3K inhibitor wortmannin increases β cell differentiation from ventral endoderm. (A-B'') Merged and single channel confocal planes of 30 hpf control (A-A'') and 1 μ M wortmannin-treated (B-B'') islets zygotically-injected with H2B-RFP mRNA and stained with CFP (β cells, green). It is noted that majority of control β cells were H2B-RFP-positive but significant portion of H2B-RFP-negative β cells (yellow arrows) were detected in wortmannin-treated embryos. (C) Quantification of DBCs (H2B-RFP-positive) and VBCs (H2B-RFP-negative) in 30 hpf DMSO-treated control ($n=12$) and 1 μ M wortmannin treated embryos ($n=15$). One-way ANOVA was used in C for statistical analysis.

Figure S9. *insaMO* does not increase β cell proliferation. (A-B'') Merged and single channel confocal projections of 1 dpf control (A-A''; $n=6$) and *insaMO*-injected (B-B''; $n=5$) *Tg(ins:CFP-NTR)* islets stained with CFP (β cells, green), phospho-Histone H3 (red), and insulin (white). (C-D'') Merged and single channel confocal planes of 1 dpf control (C-C''; $n=6$) and *insaMO*-injected (D-D''; $n=5$) *Tg(ins:CFP-NTR)* islets stained with CFP (β cells, green), EdU (red) and Insulin (white).

Figure S10. Insulin knockdown induces ectopic Pdx1 expression in ventral endoderm. Merged and single channel confocal images of 24 hpf control (A-B') and *insaMO*-injected (C-D') *Tg(ins:CFP-NTR)* islets immunostained for CFP (β cells, green), Pdx1 (red), and DNA (blue). (A) Confocal projection and (B-B') higher power magnification confocal plane of control islet. (C) Confocal projection and (D-D') higher power magnification confocal plane of *insaMO*-injected islet. Note the formation of β cells from Pdx1⁺ ventral endoderm (ve) in *insaMO*-injected embryos (yellow arrow). Abbreviation: pi, principal islet.

Figure S11. Insulin knockdown disrupts islet structure and α cell development. Confocal projections of control and *insaMO*-injected islets from *Tg(ins:CFP-NTR)* embryos immunostained for CFP (β cells, green), Glucagon (red), and DNA (blue) at 54 hpf (A,D), 80 hpf

(B,E) and 100 hpf (C,F). Islets in *insaMO*-injected embryos are dysmorphic with insulin-positive β cells aberrantly surrounding a diminished number of Glucagon-positive α cells.

Figure S12. Insulin knockdown has no effect on δ cell number or total endocrine cell number. (A,B) Confocal projections of 3 dpf control (A) and *insaMO*-injected (B) islets immunostained for Insulin (green), Somatostatin (red), and DNA (blue). (C) Quantification of somatostatin-positive cells in control ($n=5$) and *insaMO*-injected ($n=6$) embryos at 3 dpf. No significant change was evident in δ cell mass. (D) Quantification of endocrine cells in control and *insaMO*-injected embryos from 1 dpf to 4 dpf. $n \geq 7$ for all time points. (E-L) Confocal projections of control (E-H) and *insaMO* (I-L) islets in doubly transgenic *Tg(neurod:GFP); Tg(ins:dsRed)* embryos. Student's t-test was used in C and two way ANOVA was used in D to determine significance.

Figure S13. *insulin* knockdown increases α cell plasticity. (A-D) Confocal planes show control (A,C) and *insaMO*-injected (B,D) *Tg(gcga:GFP)* islets at 30 hpf (A,B) and 100 hpf (C,D) immunostained for Pdx1 (red) and DNA (blue). An increased number of double positive Gcg+ Pdx1+ cells are indicated by arrows. (E) Quantification of *gcga:GFP*+ (white), *gcga:GFP*+ Pdx1+ (gray), and Pdx1+ (red) cells in control and *insaMO*-injected embryos at 30 hpf and 100 hpf. $n \geq 7$ for all time points. (F-G''') Confocal planes showing β cell regeneration after MTZ treatment in control (F-F''') and *insaMO*-injected (G-G''') triply transgenic *Tg(ins:Flag-NTR); Tg(hs:loxp-mcherry-loxp-H2BGFP); Tg(gcga:cre)^{s962}* islets immunostained for Insulin (white), GFP (green), Glucagon (red), and DNA (blue). Red arrows indicate H2B-GFP+ Glucagon+ cells, which have retained α cell character, while white arrows indicate H2B-GFP+ Glucagon- cells, which have lost α cell character during β cell regeneration. (H) Percentage of the H2B-GFP-positive cell population that is Gcg-negative in control ($n=7$) and *insaMO*-injected regenerating ($n=13$) islets. More lineage-labeled α cells lost glucagon expression in *insaMO*-injected islets than in control, suggesting increased plasticity. Student's t-test was used in H to determine significance.

Figure S14. Transplanted endoderm-committed blastomeres (ECBs) can differentiate into pancreatic endocrine cells in β cell ablated host larvae. (A-C') Merged and single channel confocal planes of chimeras composed of *Tg(sox17:GFP)* ECBs transplanted into β cell-ablated host larvae, shown at 2 days post transplantation (dpt)/6 dpf. Chimeras were immunostained for

GFP (green), Insulin (red), Glucagon (white), and DAPI (blue). (A,B) Control donor ECBs, and (C) *dnIRS2-GFP* mRNA-injected ECBs. With insulin signaling blockade, insulin+ β cell generation was increased in donor ECBs, while Glucagon+ α cell generation was decreased.

Figure S15. Transplantation of ECBs influences host β cell regeneration in the principal islet. (A-C) Confocal projections of host-derived regenerating principal islets within chimeras at 2 days post ablation. Chimera composition was: (A-A'') Sham donor control without transplantation (B-B''); control donor *Tg(sox17:GFP)* ECBs; and (C-C'') *dnIRS2-GFP* mRNA-injected donor *Tg(sox17:GFP)* ECBs. Chimeras were immunostained for Insulin (red), Glucagon (white), and DNA (blue). Regeneration of β cells was increased in the principal islet of the host when insulin signaling was blocked by *dnIRS2-GFP* in the transplanted ECBs.

Fig S1.
Ye et al., DBIO-15-220

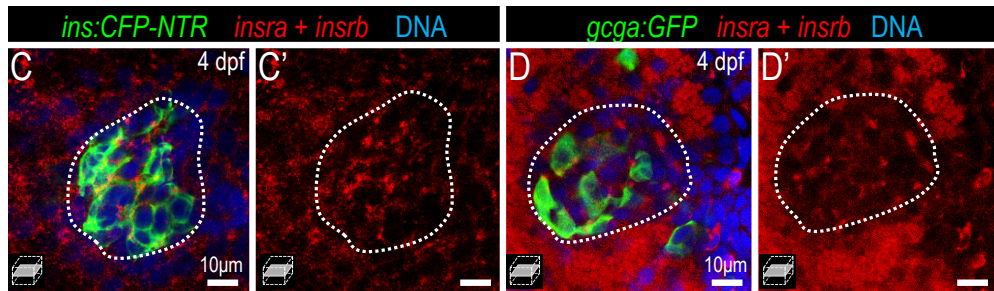
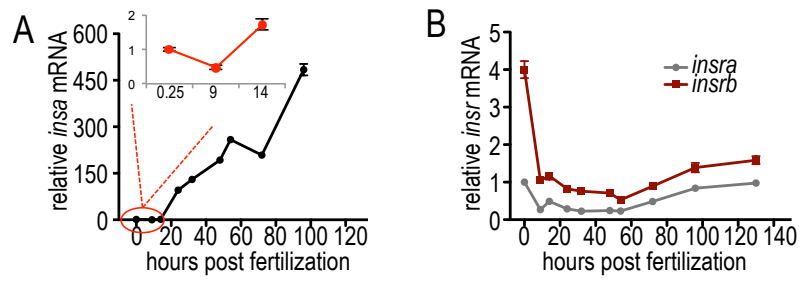


Fig S2.
Ye et al., DBIO-15-220

A dnIRS2-EGFP PH domain PTB domain EGFP

```

MASPPPTGGQLISDMTVKNNNHVKKCGYLRKQKHGHRFFVLREPS
DGSRARLEYESEKKWKNKSAKRVIPLDSCLNINKRADAKHKHLI
ALYTKDEYFAVATENEQEQEDWFTVLTDLMNEGKVSDGSASNSASS
LVGFDEANYGVITPVTAAYKEVWQVNLKSKGLGQSRNLTVVYRLCL
SSRTISFVKLNTENASVILQLMNIRRCGHSDSFFFIEVGRSASIGP
GELWMOADDSVVAQNIHETILEAMKAMKEMSEFRPRSKSQSSGTNP
ISVPTRRHFNNLPPSQTGLPRRSRTDSMAAMVSKGEELFTGVVPIIL
VELDGDVNGHKFSVSGEGEGDATYGKLTLLKFICTTGKLPVPWPTLV
TTLTYGVQCFSRYPDHMKQHDFFKSAMPEGYVQERTIFFKDDGNYK
TRAEVKFEGDTLVNRIELKGIDFKEDGNILGHKLEYNYNSHNVYIM
ADKQKNGIKVNFKIRHNIEDGSVQLADHYQONTPIGDGPVLLPDNH
YLSTQSALS KDPNEKRDMVLLFVTAAGITLGMDELYK*
    
```

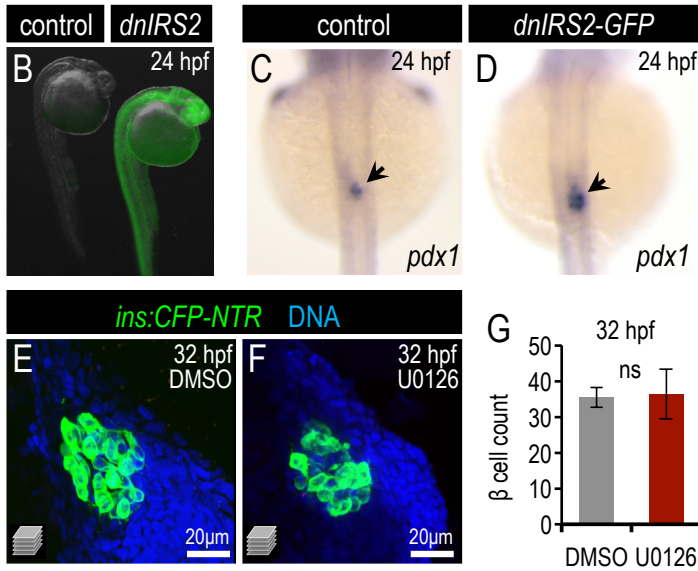


Fig S3.
Ye et al., DBIO-15-220

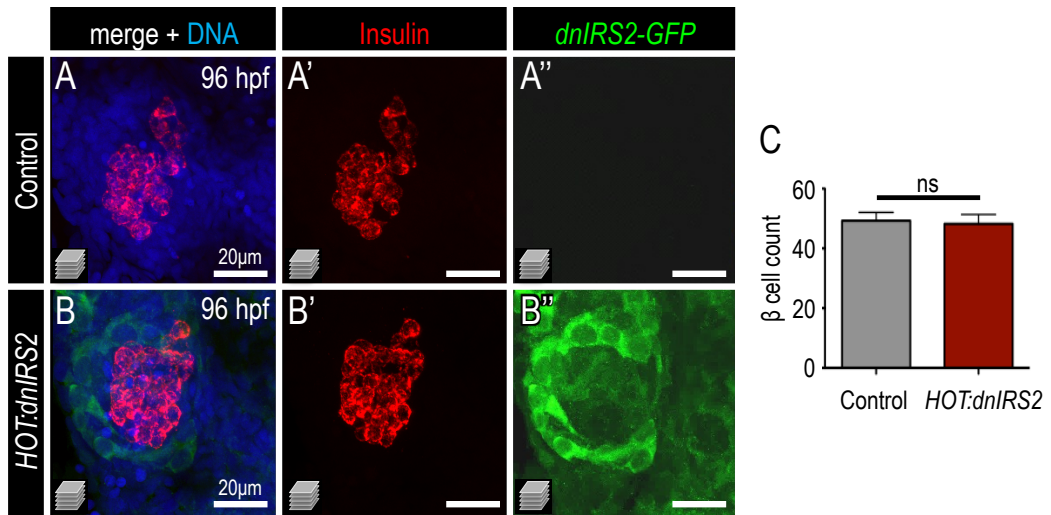


Fig S4.
Ye et al., DBIO-15-220

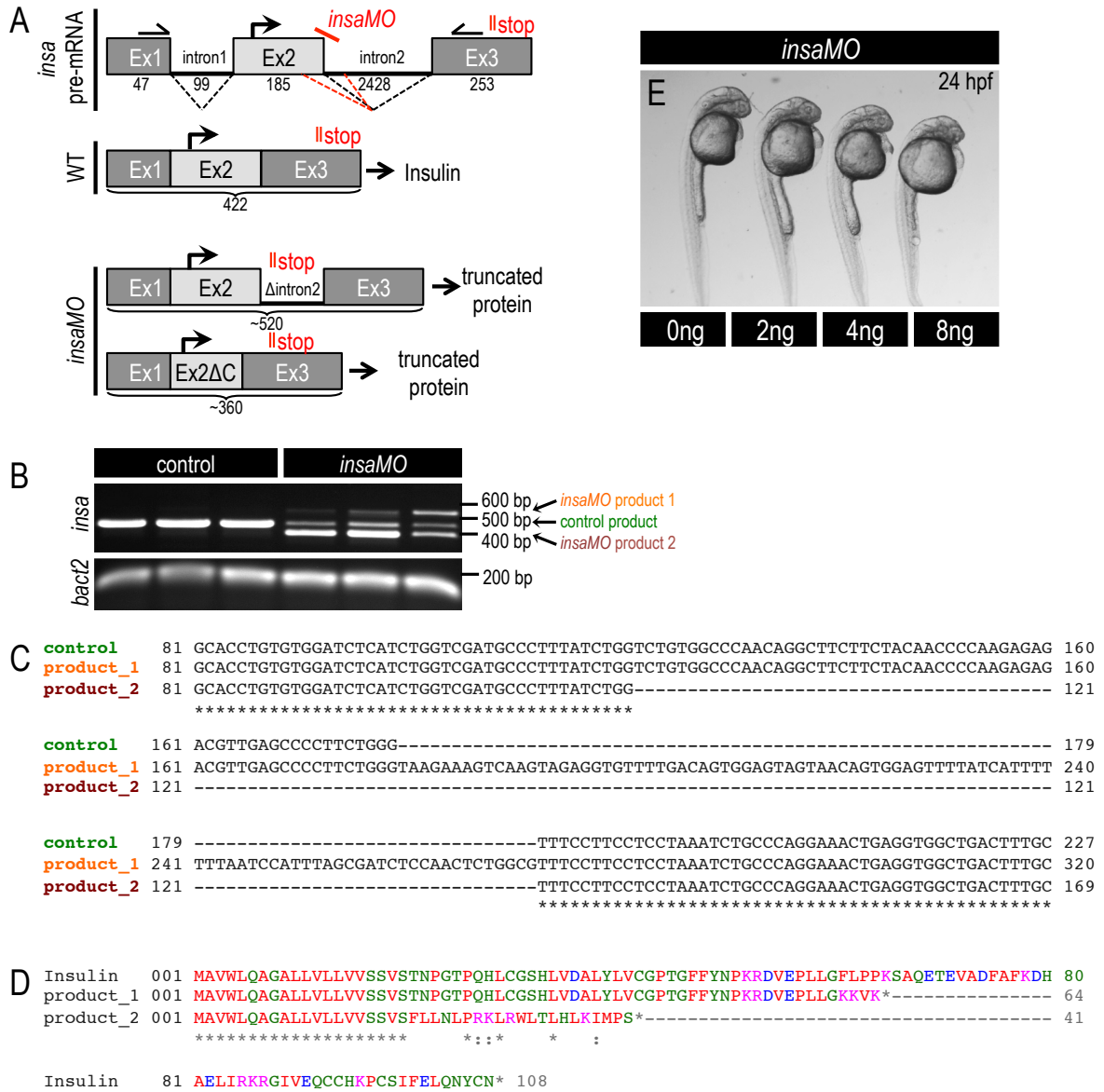


Fig S5.
Ye et al., DBIO-15-220

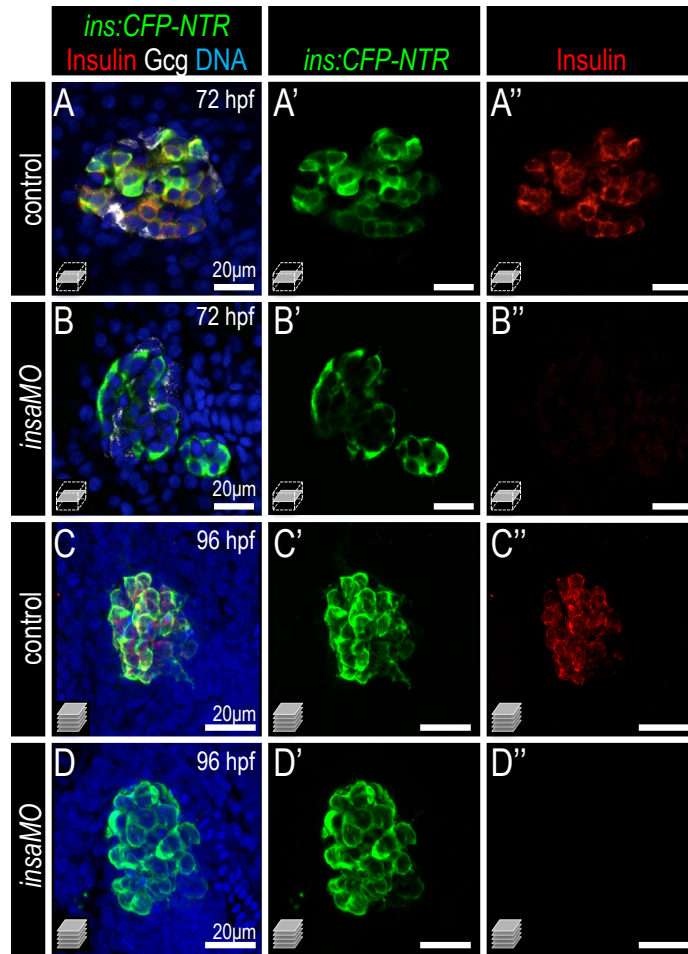


Fig S6.
Ye et al., DBIO-15-220

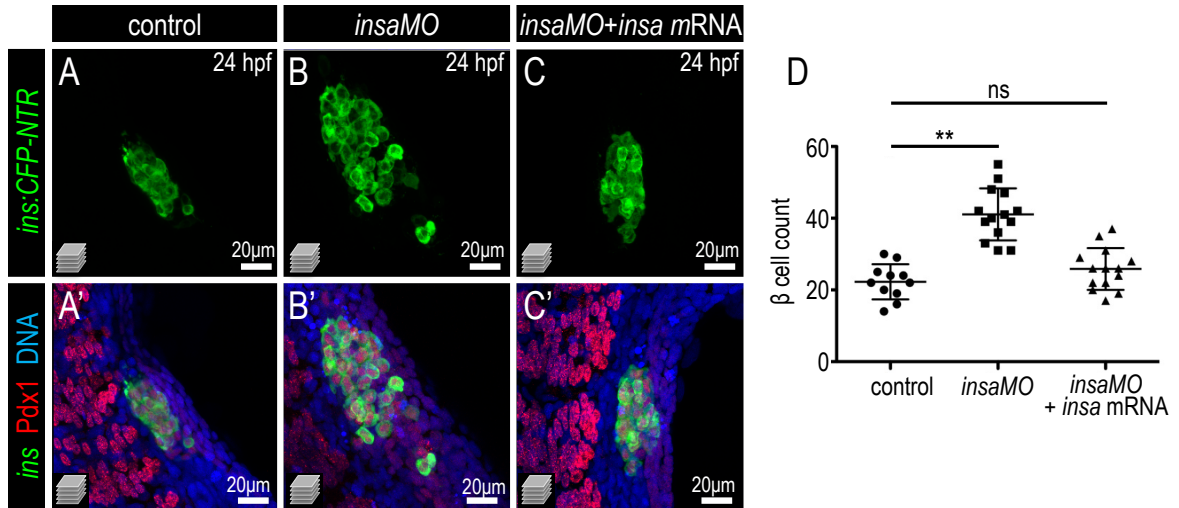


Fig S7.
Ye et al., DBIO-15-220

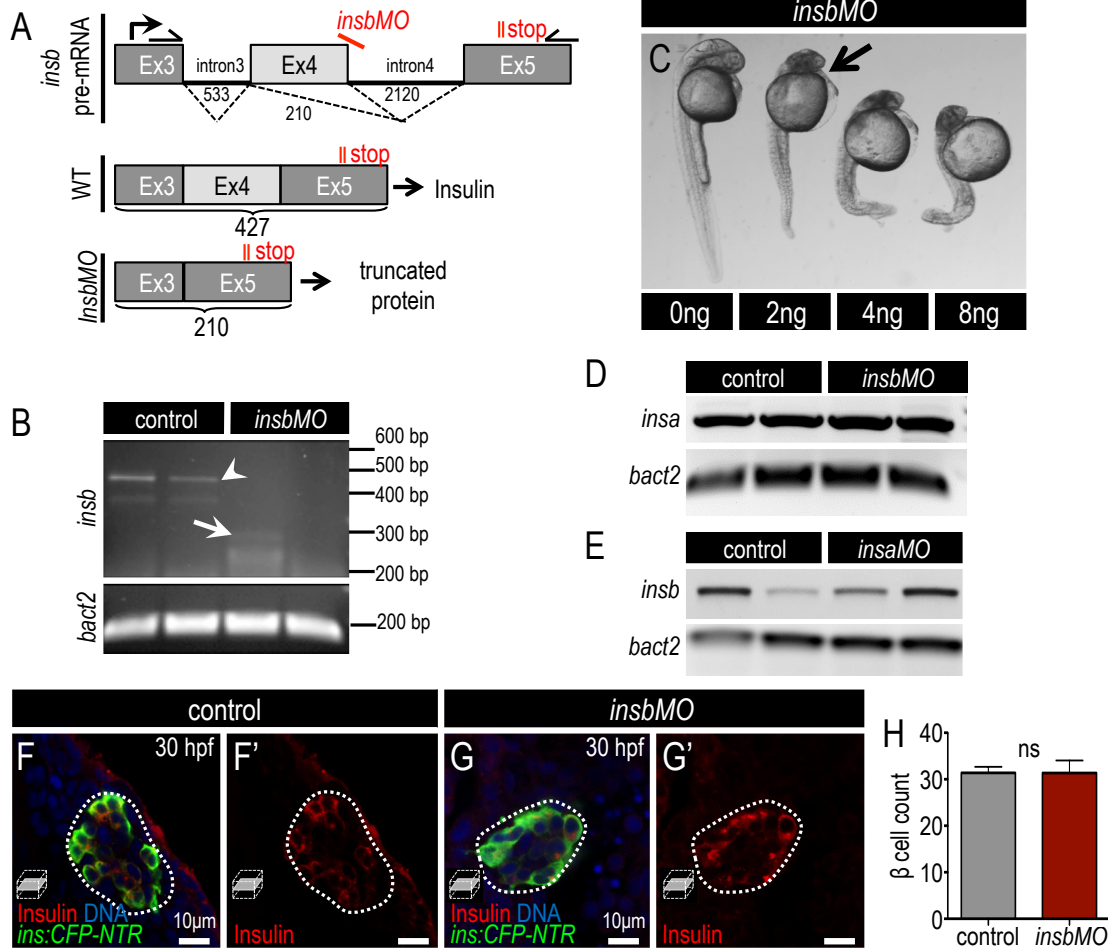


Fig S8.
Ye et al., DBIO-15-220

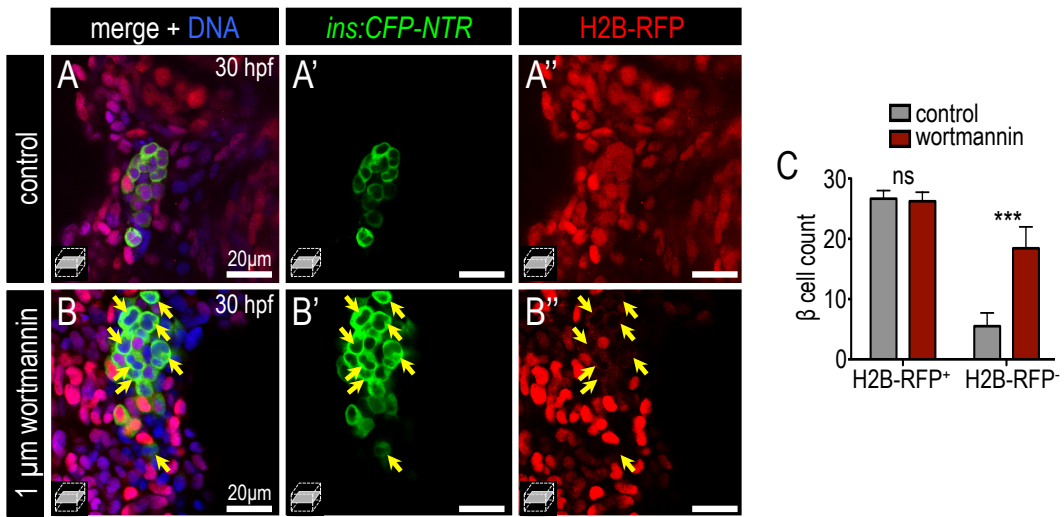


Fig S9.
Ye et al., DBIO-15-220

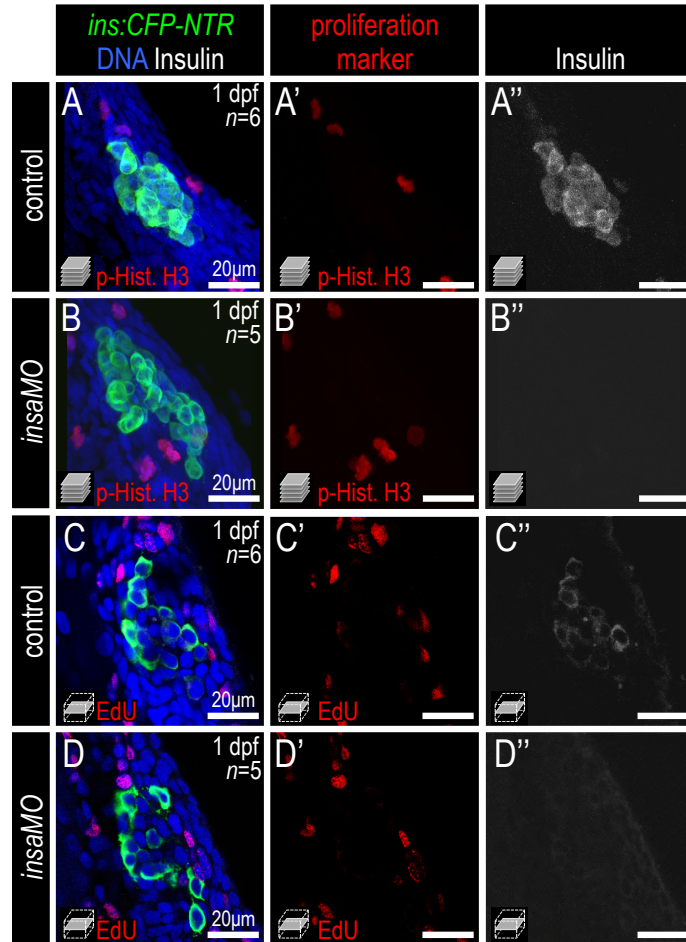


Fig S10.
Ye et al., DBIO-15-220

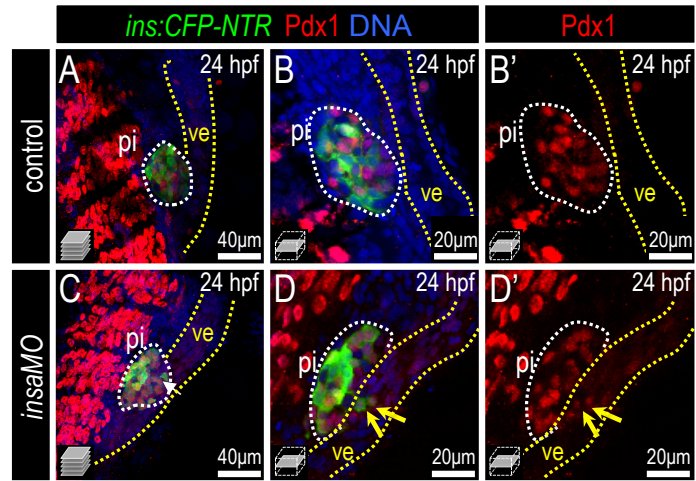


Fig S11.
Ye et al., DBIO-15-220

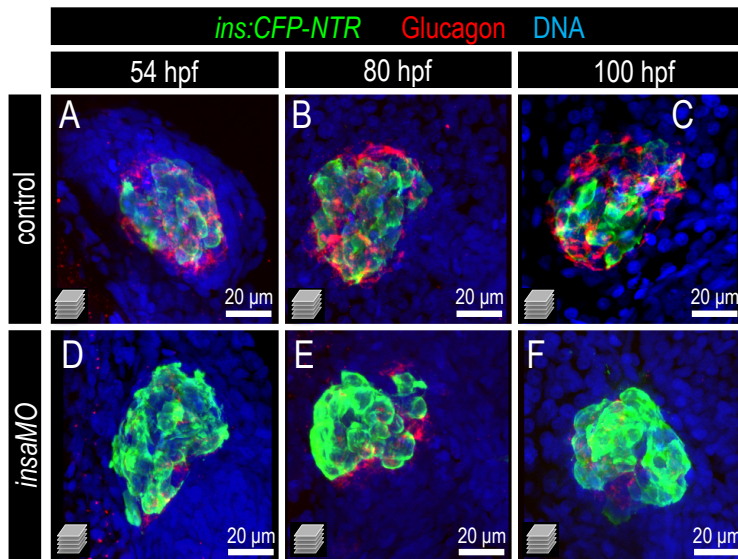


Fig S12.
Ye et al., DBIO-15-220

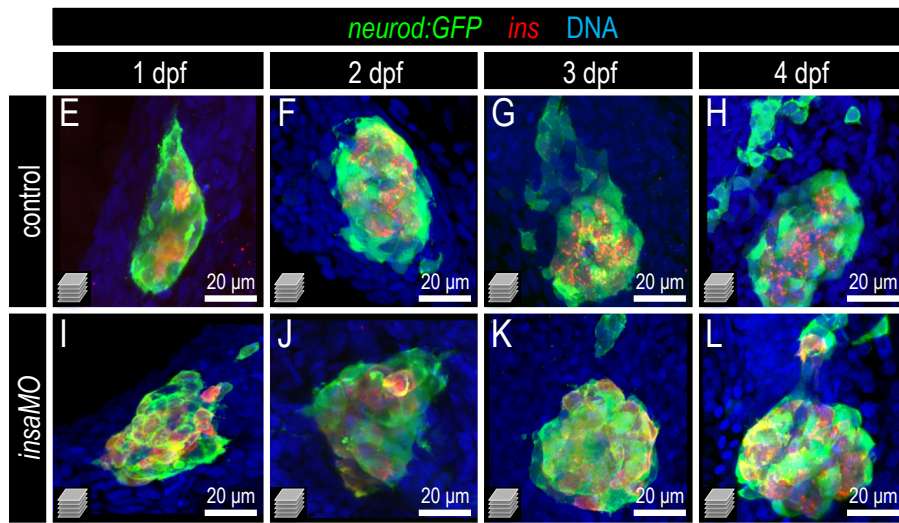
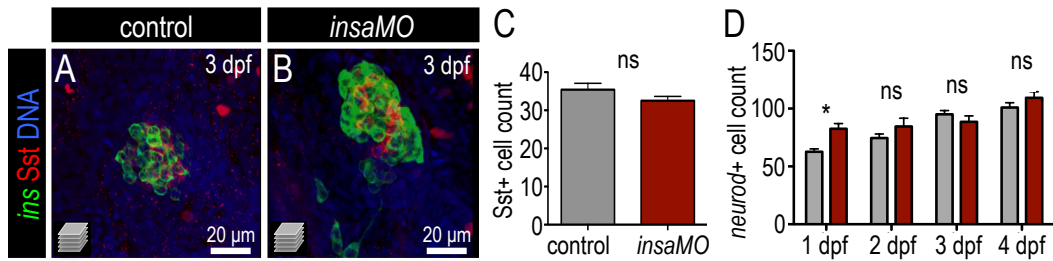


Fig S13.
Ye et al., DBIO-15-220

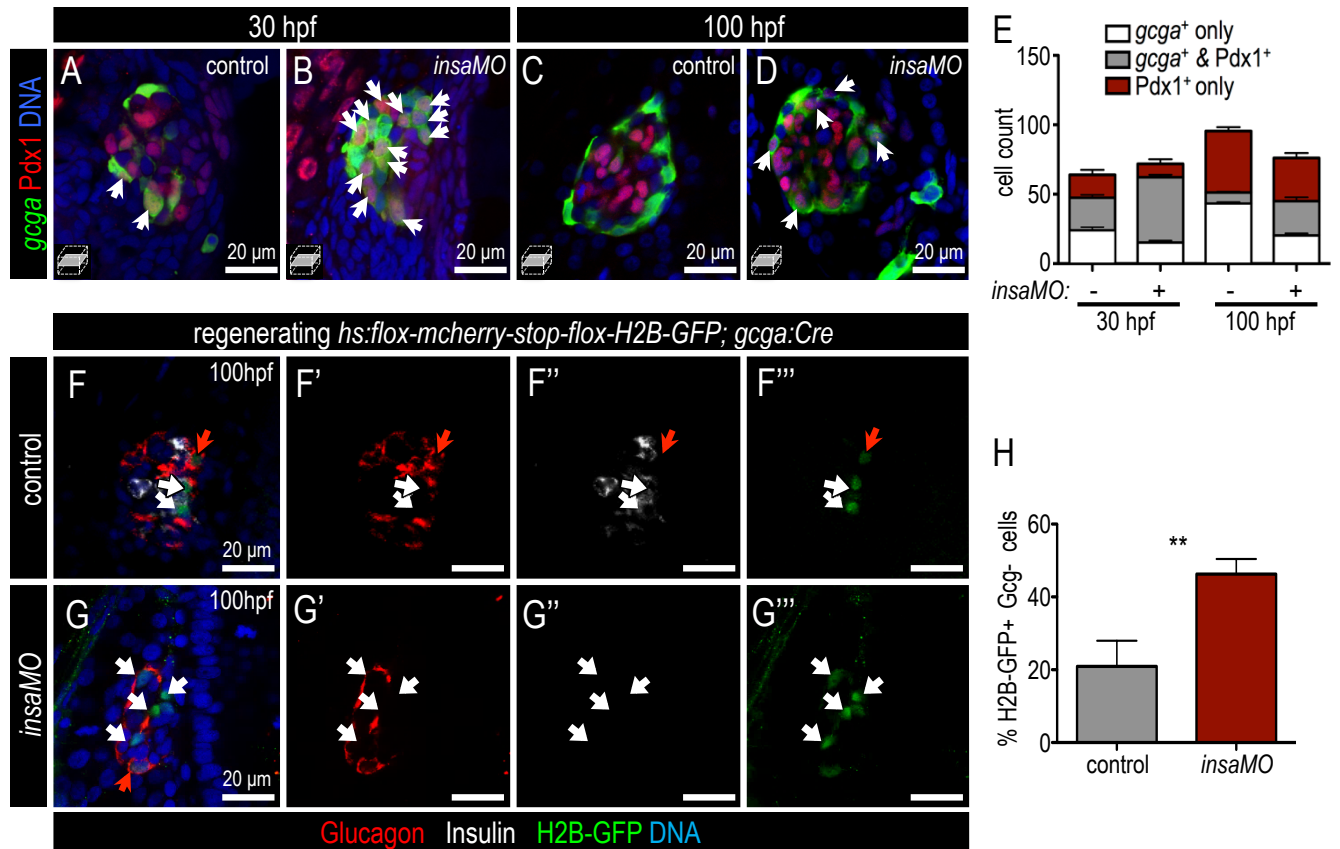


Fig S14.
Ye et al., DBIO-15-220

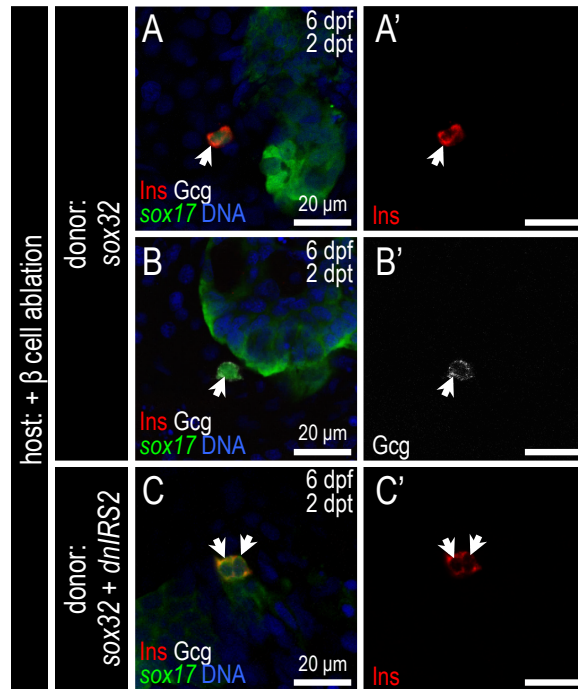


Fig S15.
Ye et al., DBIO-15-220

